Chemical Science

ROYAL SOCIETY OF CHEMISTRY

EDGE ARTICLE

View Article Online
View Journal | View Issue

Cite this: *Chem. Sci.*, 2021, **12**, 15528

All publication charges for this article have been paid for by the Royal Society of Chemistry

Received 26th August 2021
Accepted 21st November 2021

DOI: 10.1039/d1sc04728k

rsc.li/chemical-science

Adsorptive separation of cyclohexanol and cyclohexanone by nonporous adaptive crystals of RhombicArene†

Yongye Zhao, Hongyan Xiao, Chen-Ho Tung, Li-Zhu Wu and Huan Cong *

As feedstock chemicals with similar boiling points, cyclohexanol (**CHOL**) and cyclohexanone (**CHON**) are often obtained as mixtures during production processes. Separation of mixed **CHOL** and **CHON** is important but energy-consuming by distillation. Here we report the development of a new macrocycle RhombicArene, which forms a host–guest complex with **CHON** through C–H···π interactions and hydrogen bonds. The nonporous adaptive crystals of RhombicArene exhibit excellent capability for rapid (30 minutes), exclusive (>99.9%), and recyclable vapor adsorption of **CHON** in the presence of **CHOL** under mild and user-friendly conditions.

Introduction

Cyclohexanol (**CHOL**) and cyclohexanone (**CHON**), precursors for caprolactam and adipic acid, are vital feedstock chemicals for the production of nylons. In addition, **CHOL** serves as an emulsion stabilizer and a raw material for plasticizers, and **CHON** is widely used as a solvent for resins and paints.[1] Industrial preparations of **CHOL** and **CHON** entail oxidation of cyclohexane or hydrogenation of phenol.[2] Alternatively, hydration of cyclohexene is developed to afford **CHOL**[3] which can further be converted to **CHON** by oxidation (Fig. 1a).[4] During the above production processes, **CHOL** and **CHON** are inevitably obtained as mixtures, which are known as KA-oil. Due to very close boiling points, mixed **CHOL** and **CHON** are energy-consuming to purify by distillation,[5] thereby the development of alternative methods for separation is of significant importance.

Recently, macrocycle-based nonporous adaptive crystals (NACs) have emerged as efficient and selective adsorbents for mixed organic vapors with similar boiling points.[6] The high selectivity of the NAC strategy offers potential for economical and environmentally friendly separation of organic vapors, and stems from the deliberately designed macrocycles whose adaptive skeletons can provide noncovalent interactions to recognize certain guest molecules. Specifically, successful examples of NAC materials often employ electron-rich arene-based macrocycles, functioning as sources for C–H···π interactions.[7] Although adsorptions of single-component **CHOL** or **CHON** have been reported using adsorbent materials, their adsorptive separation remains a challenging goal thus far.[8] In view of the functional group difference between **CHON** and **CHOL**, we envisioned that the development of a hybrid macrocycle containing electron-rich arenes and *endo* hydrogen-bonding moieties[9] would be helpful to differentiate these two molecules during adsorption.

Here we report a novel macrocycle named RhombicArene (**1**, Fig. 1b) as an adaptive and selective adsorbent for **CHON**. The structural design of the C_2-symmetrical **1** features methylene-bridged *para*-dimethoxy arenes adopted from pillararenes,[10] as well as two octahydrobinaphthol (H_8-**BINOL**) subunits as linkers and in-cavity hydrogen-bonding sites.[11] The crystal

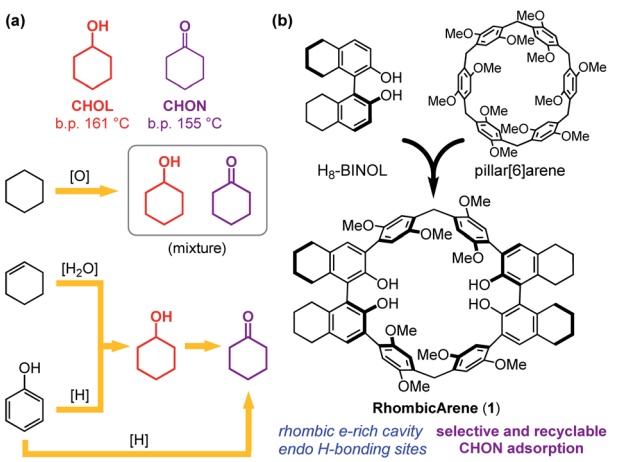

Fig. 1 (a) Preparative routes of cyclohexanol and cyclohexanone. (b) Molecular design of RhombicArene (**1**).

Key Laboratory of Photochemical Conversion and Optoelectronic Materials, Key Laboratory of Bio-inspired Materials and Interfacial Science, Technical Institute of Physics and Chemistry, Chinese Academy of Sciences & School of Future Technology, University of Chinese Academy of Sciences, Beijing, 100190, China. E-mail: hcong@mail.ipc.ac.cn

† Electronic supplementary information (ESI) available. CCDC 2067429 and 2067432. For ESI and crystallographic data in CIF or other electronic format see DOI: 10.1039/d1sc04728k

structure reveals a host–guest complex between **1** and **CHON** through C–H···π interactions and hydrogen bonds, demonstrating the adaptivity of **1** in the crystalline state. The activated crystals of **1** exhibit rapid, exclusive, and recyclable vapor adsorption of **CHON** in the presence of **CHOL**. Furthermore, treatment of a **CHOL**/**CHON** mixture (98 : 2) with **1** at 30 °C for just 30 minutes can produce high-purity liquid **CHOL** (99.7% by GC analysis) through selective adsorption of **CHON**, indicating attractive potential toward efficient and greener purification.

Results and discussion

Synthesis and crystal structure

The concise synthesis of **1** entails three steps from **H_8-BINOL**, a widely useful building block, both enantiomers of which are commercially available.[12] Starting with a single enantiomer of **H_8-BINOL**, iodination followed by cross-coupling smoothly installed the electron-rich aryl moieties, affording precursor **2**. Initially, the desired macrocycle **1** was prepared, albeit with low yield, employing Friedel–Crafts-type condensation between **2** and paraformaldehyde promoted by Lewis acid (Table S1†).[13] During the subsequent investigation, examination of the crystal structure of **CHON@1** confirmed the host–guest interactions inside **1**'s cavity (*cf.* Fig. 3c), which inspired us to revisit the preparation. We reasoned that a **CHON** analogue bearing two ketone moieties could hold two molecules of **2** in proximity, and serve as a noncovalent template to facilitate the macrocyclization step.[14] Indeed, improved yield could be obtained upon addition of 0.5 equivalent of 1,4-cyclohexanedione (Fig. 2a and Table S2†). The overall three-step yield of the macrocycle **1** is 16%.

X-ray crystallographic analysis of **1** confirmed its rhombic-shaped cavity with the size of 1.0 nm, and indicated four intramolecular hydrogen bonds within one molecule (Fig. 2b). The hydrogen bond between each hydroxyl group and the methoxy group of the adjacent arene moiety could enable the *para*-dimethoxy arenes not only to maintain the upright conformation with enhanced rigidity, but also to adopt the same orientation because all **H_8-BINOL** subunits carried single chiral configuration. The crystal structure of **1** would provide a clue to explain the unsuccessful macrocyclization employing racemic precursor **2** (Table S3†), which may lead to mismatched orientations of the *para*-dimethoxy arenes. Examination of the molecular packing of **1** in the crystalline state revealed that the macrocycles adopt two orientations linked by multiple intermolecular C–H···π interactions (Fig. 2c). Each unit cell contains a pair of macrocycles with complementary orientations, and further packs into staggered layers with brick-wall-like patterns. Although the neighboring layers block each other along the axes of the unit cell, long-range channels exist in the diagonal direction (Fig. 2d).

Single-component vapor adsorption

The crystallized macrocycle **1** was activated by heating at 50 °C under reduced pressure. The resulting desolvated white powder was proved to be nonporous, as indicated by its minimal Brunauer–Emmett–Teller (BET) surface area (Fig. S5†). Single-

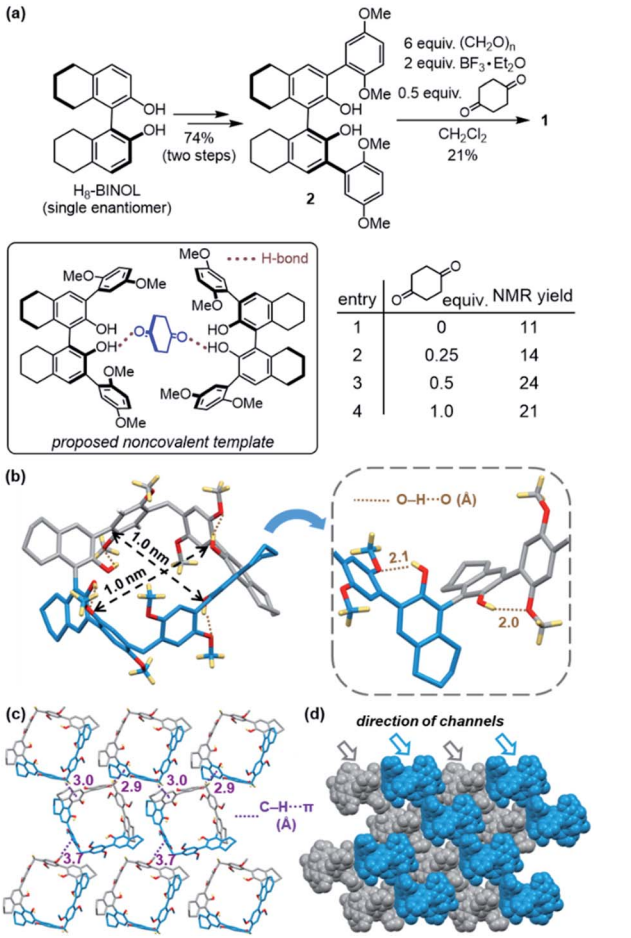

Fig. 2 (a) Synthesis of RhombicArene (**1**). (b) Crystal structure of **1**. (c) Top-view and (d) side-view of molecular packing of **1** in the crystalline state. Solvents and part of hydrogen atoms were omitted for clarity.

component solid–vapor uptake experiments using activated **1** confirmed the adsorptive capability of **CHON**, with negligible adsorption of **CHOL** even after prolonged time at 30 °C (Fig. 3a and S6†). Notably, it takes less than 30 min for the **CHON** adsorption to reach saturation, which is significantly faster compared to most NAC materials reported to date.[6,15] Powder X-ray diffraction analysis (PXRD, Fig. 3b and S7†) revealed the crystallinity of the activated **1**, whose PXRD patterns matched with the simulated results based on the crystal structure of **1**, suggesting comparable molecular packing modes. Consistent with the single-component adsorption experiments, the PXRD patterns of **1** showed little changes after treatment with **CHOL** vapor for 3 hours at 30 °C, whereas distinct pattern changes were observed upon in contact with **CHON** vapor for 30 min at the same temperature. Moreover, the new PXRD patterns resemble the simulated patterns of the crystals of **CHON@1**, which were obtained by slow diffusion of diethyl ether into a cyclohexanone solution of **1**.

The crystal structure of **CHON@1** showed the formation of a 1 : 1 host–guest complex (Fig. 3c). One **CHON** molecule, adopting a chair-like conformation, is located inside each cavity of **1**. The host–guest supramolecular structure was stabilized by

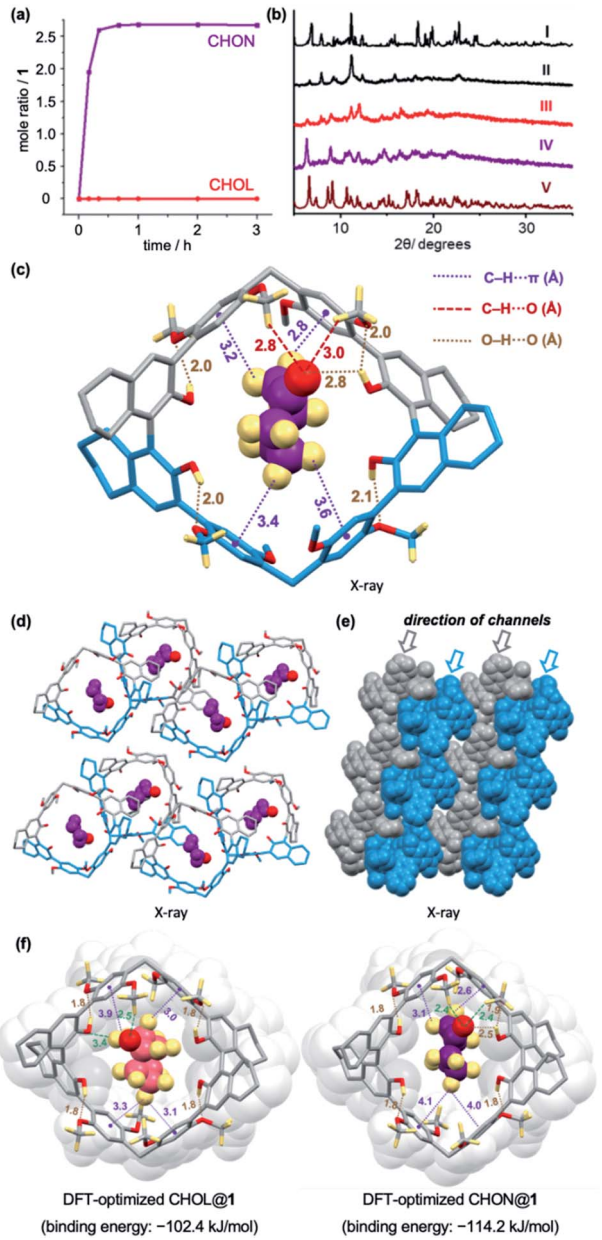

Fig. 3 (a) Time-dependent single-component solid–vapor adsorption plots of the activated crystals of **1** at 30 °C. (b) PXRD patterns of **1** under different conditions: (I) simulated from single-crystal structure of **1**, (II) activated **1**, (III) after treatment with **CHOL** vapor, (IV) after treatment with **CHON** vapor, (V) simulated from single-crystal structure of **CHON@1**. (c) Crystal structure of **CHON@1** showing host–guest interactions. (d) Top-view and (e) side-view of molecular packing of **CHON@1** in the crystalline state. Solvents and part of hydrogen atoms were omitted for clarity. (f) Computationally optimized structures for **CHOL@1** and **CHON@1**.

the hydrogen bond between one of the macrocycle's hydroxyl groups and the oxygen atom of the ketone, along with multiple C–H···π and C–H···O interactions contributed by the *para*-dimethoxy arene moieties. Induced by guest inclusion, slight distortions of the macrocyclic skeleton were observed (Fig. S3 and S4†). In addition, **CHON@1** exhibits different molecular packing (Fig. 3d and e) compared to the crystals of **1** by itself, demonstrating the adaptive feature of the macrocyclic host. Besides **CHON** and macrocycle **1**, each unit cell of **CHON@1** also contains a Et_2O molecule and a disordered molecule (which cannot be well resolved, likely another Et_2O molecule, Fig. S4b†) occupying the voids outside the macrocyclic cavity. In comparison, the vapor adsorption experiments employ the desolvated solid of **1**, in which the voids in the crystalline solid are unoccupied and available for adsorption.[6g,i] Such difference may account for the higher molar ratio of **CHON** : **1** observed in the vapor adsorption experiment than in the crystal structure of **CHON@1**. Indeed, similar observations regarding the guest/macrocycle molar ratios have been reported for other NAC materials in the literature.[6o,r] Accordingly, the preference for **CHON** adsorption would be contributed by both interstitial space and macrocyclic cavities of the adaptive crystals of **1**. While the mechanism at the molecular level for the highly selective **CHON** adsorption would warrant future investigation, the observed similarities between the simulated and experimental PXRD patterns (Fig. 3b) implied the adaptive morphology transformation as a result of **CHON** vapor uptake. The structural details and molecular packing of **CHON@1** would, in turn, be helpful to elucidate the noncovalent interactions accompanying **CHON** adsorption.

In addition, DFT calculation was performed to optimize the structures of **CHOL@1** and **CHON@1** (Fig. 3f). Because the hydroxyl group of **CHOL** takes an equatorial position of the chair conformation of the cyclohexane ring, **CHOL** and **CHON** adopt different orientations inside the macrocyclic cavity. Hence, the DFT-optimized structure of **CHOL@1** indicates a weaker hydrogen bond (relative to that in **CHON@1**) with the O–H···O length of 3.4 Å between the hydroxyl group of **CHOL** and one of the oxygen atoms located at the macrocycle's **H$_8$-BINOL** subunit. The results indicated that the binding energy of **CHOL@1** is 11.8 kJ mol^{-1} less than that of **CHON@1**, which is thermodynamically consistent with the higher selectivity for **CHON**. Additionally, in view of the calculated exothermic **CHOL** binding, the observed minimal **CHOL** adsorption shown in Fig. 3a may be due to kinetic barriers.

Mixed CHOL/CHON vapor adsorption

Encouraged by the single-component adsorption performance, we evaluated the capability of **1** as a selective adsorbent for mixed vapor (Fig. 4a). When subjected to the mixed vapor of **CHOL** and **CHON** at 30 °C (v/v 23 : 77 based on Antoine equation, Fig. S17†),[16] the activated crystals of **1** exhibited exclusive adsorption of **CHON**, with the purity of >99.9% by GC analysis of the adsorbed **CHON** (Fig. 4b and S15†). Time-dependent vapor uptake plot indicated rapid saturation for **CHON** with minimal **CHOL** adsorption, maintaining the same features of the single-component adsorptions (Fig. S12† *vs.* Fig. 3a). In addition, PXRD analysis of **1** after adsorption of the mixed vapor also showed resembling patterns compared to those after single-component adsorption of **CHON** (Fig. S13†). After vapor adsorption, the activated crystals of **1** could be easily regenerated through heating under vacuum, and the recyclability test

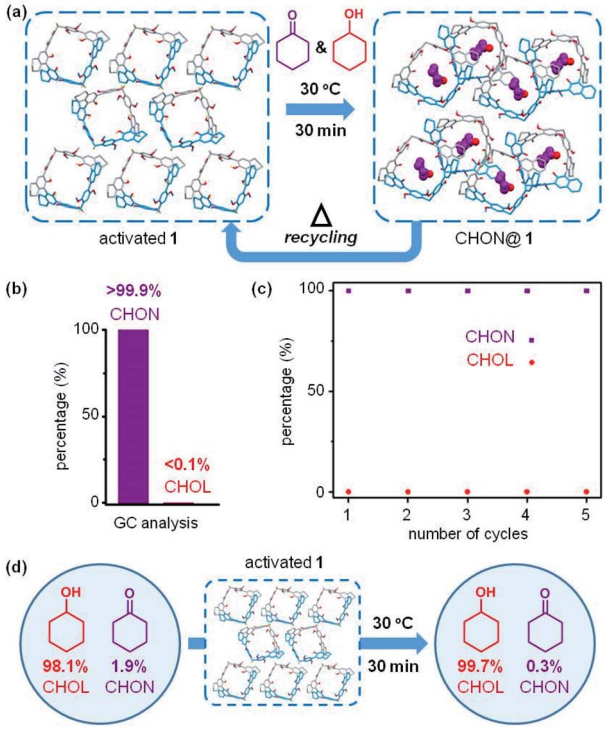

Fig. 4 (a) Solid–vapor adsorption for CHOL/CHON mixed vapor employing activated crystals of 1. (b) Relative contents of CHOL and CHON adsorbed by 1 at 30 °C after 30 min measured by gas chromatography. (c) Recycling performance of 1. (d) Facile purity enhancement of liquid CHOL after the solid–vapor adsorptive treatment by activated crystals of 1.

of **1** by five adsorption–activation cycles confirmed the robust separative performance for **CHOL**/**CHON** mixed vapor (Fig. 4c).

Since ultra-pure chemicals are of considerable practical and commercial value, we next investigated the utility of **1** to remove trace **CHON** from liquid **CHOL** through solid–vapor adsorption. Upon exposure of 98 : 2 liquid **CHOL**/**CHON** (0.05 mL, containing 1.9% **CHON** impurity) to activated crystals of **1** (9 mg) in a sealed container at 30 °C, the **CHON** content dramatically reduced to 0.3% as revealed by GC analysis (Fig. 4d and S18†). During the experiment, the activated macrocycle **1** does not directly contact with the liquid **CHOL**, leading to user-friendly operations and easy separation of adsorbent. Notably, the purity enhancement of liquid **CHOL** could be achieved in 30 minutes, demonstrating the facile and selective **CHON** adsorption even at very low **CHON** content.

Conclusions

In summary, we have designed and synthesized a new macrocycle RhombicArene (**1**). The adaptive cavity of **1** is surrounded by electron-rich *para*-dimethoxy arenes and *endo* hydroxyl moieties, enabling the host–guest complexation with **CHON** through C–H···π interactions and hydrogen bonds, respectively. The activated crystals of **1** have been successfully used as a highly selective, recyclable, and facile adsorbent for **CHON**, at the same time showing minimal adsorption for **CHOL**. The properties and utility of **1** demonstrate the advantages of macrocycle-based adaptive adsorbent to distinguish organic vapors with minor structural differences, showing promising potential for energy-saving separation and high-grade chemical purification.

Data availability

The crystallographic data for **1** and **CHON@1** have been deposited at CCDC with deposition numbers 2067429 and 2067432, respectively. The data can be obtained *via* www.ccdc.cam.ac.uk/structures.

Author contributions

H. C. and Y. Z. proposed the project and designed the experiments. Y. Z. carried out the experiments. H. X. performed DFT calculations. H. C., Y. Z., C.-H. T. and L.-Z. W. analyzed data. H. C. and L.-Z. W. wrote the manuscript with inputs from all authors. H.C. directed the project with critical consultation from C.-H. T. and L.-Z. W.

Conflicts of interest

There are no conflicts to declare.

Acknowledgements

Financial support from the National Natural Science Foundation of China (21672227, 21922113, 21988102, 22071257), the Strategic Priority Research Program of Chinese Academy of Sciences (XDB17000000), the National Key Research and Development Program of China (2017YFA0206903), K. C. Wong Education Foundation and the TIPC Director's Fund is gratefully acknowledged. We thank Profs Congyang Wang (ICCAS), Zhaohui Wang, Shaoguang Zhang and Bi-Jie Li (Tsinghua University); Drs Xiaodi Yang (Shanghai University of Traditional Chinese Medicine) and Wen Zhou (Peking University); Mr Shu Niu and Lijie Zhan are acknowledged for the help with compound characterizations.

References

1 (*a*) W. B. Fisher and J. F. Van Peppen, in *Kirk-Othmer Encyclopedia of Chemical Technology,* John Wiley & Sons, Inc., New York, 2000; (*b*) M. T. Musser, in *Ullmann's Encyclopedia of Industrial Chemistry*, Wiley-VCH Verlag GmbH & Co. KGaA, 2000.

2 (*a*) U. Schuchardt, D. Cardoso, R. Sercheli, R. Pereira, R. S. Da Cruz, M. C. Guerreiro, D. Mandelli, E. V. Spinacé and E. L. Pires, *Appl. Catal., A*, 2001, **211**, 1; (*b*) I. Dodgson, K. Griffin, G. Barberis, F. Pignataro and G. Tauszik, *Chem. Ind.*, 1989, 830; (*c*) H. Liu, T. Jiang, B. Han, S. Liang and Y. Zhou, *Science*, 2009, **326**, 1250.

3 (*a*) O. Mitsui and Y. Fukuoka, *US Pat.*, 4588846, 1986; (*b*) F. Steyer and Z. W. Qi, *Chem. Eng. Sci.*, 2002, **57**, 1511; (*c*)

T. Qiu, C.-H. Kuang, C.-G. Li, X.-W. Zhang and X.-D. Wang, *Ind. Eng. Chem. Res.*, 2013, **52**, 8139.

4 (*a*) V. Z. Fridman and A. A. Davydov, *J. Catal.*, 2000, **195**, 20; (*b*) B. M. Nagaraja, V. S. Kumar, V. Shashikala, A. H. Padmasri, S. S. Reddy, B. D. Raju and K. S. R. Rao, *J. Mol. Catal. A: Chem.*, 2004, **223**, 339.

5 H. Wang, C. Cui, H. Lyu and J. Sun, *Sep. Purif. Technol.*, 2019, **211**, 279.

6 (*a*) J. L. Atwood, L. J. Barbour, A. Jerga and B. L. Schottel, *Science*, 2002, **298**, 1000; (*b*) P. K. Thallapally, B. P. McGrail, S. J. Dalgarno, H. T. Schaef, J. Tian and J. L. Atwood, *Nat. Mater.*, 2008, **7**, 146; (*c*) K. Jie, M. Liu, Y. Zhou, M. A. Little, S. Bonakala, S. Y. Chong, A. Stephenson, L. Chen, F. Huang and A. I. Cooper, *J. Am. Chem. Soc.*, 2017, **139**, 2908; (*d*) T. Ogoshi, Y. Shimada, Y. Sakata, S. Akine and T.-a. Yamagishi, *J. Am. Chem. Soc.*, 2017, **139**, 5664; (*e*) K. Jie, M. Liu, Y. Zhou, M. A. Little, A. Pulido, S. Y. Chong, A. Stephenson, A. R. Hughes, F. Sakakibara, T. Ogoshi, F. Blanc, G. M. Day, F. Huang and A. I. Cooper, *J. Am. Chem. Soc.*, 2018, **140**, 6921; (*f*) K. Jie, Y. Zhou, E. Li, R. Zhao and F. Huang, *Angew. Chem., Int. Ed.*, 2018, **57**, 12845; (*g*) J.-R. Wu and Y.-W. Yang, *J. Am. Chem. Soc.*, 2019, **141**, 12280; (*h*) Y. Wang, K. Xu, B. Li, L. Cui, J. Li, X. Jia, H. Zhao, J. Fang and C. Li, *Angew. Chem., Int. Ed.*, 2019, **58**, 10281; (*i*) J. Zhou, G. Yu, Q. Li, M. Wang and F. Huang, *J. Am. Chem. Soc.*, 2020, **142**, 2228; (*j*) X. Sheng, E. Li, Y. Zhou, R. Zhao, W. Zhu and F. Huang, *J. Am. Chem. Soc.*, 2020, **142**, 6360; (*k*) Y. Zhou, K. Jie, R. Zhao, E. Li and F. Huang, *J. Am. Chem. Soc.*, 2020, **142**, 6957; (*l*) J.-R. Wu, B. Li and Y.-W. Yang, *Angew. Chem., Int. Ed.*, 2020, **59**, 2251; (*m*) H. Zuilhof, K. Samanta, W. Yang, X. Wan, T. U. Thikekar, Y. Chao, S. Li, K. Du, J. Xu, Y. Gao and A. C.-H. Sue, *Angew. Chem., Int. Ed.*, 2020, **59**, 3994; (*n*) Q. Li, K. Jie and F. Huang, *Angew. Chem., Int. Ed.*, 2020, **59**, 5355; (*o*) H. Yao, Y.-M. Wang, M. Quan, M. U. Farooq, L.-P. Yang and W. Jiang, *Angew. Chem., Int. Ed.*, 2020, **59**, 19945; (*p*) A. Dey, S. Chand, B. Maity, P. M. Bhatt, M. Ghosh, L. Cavallo, M. Eddaoudi and N. M. Khashab, *J. Am. Chem. Soc.*, 2021, **143**, 4090; (*q*) W. Zhu, E. Li and F. Huang, *ACS Appl. Mater. Interfaces*, 2021, **13**, 7370; (*r*) D. Luo, J. Tian, J. L. Sessler and X. Chi, *J. Am. Chem. Soc.*, 2021, **143**, 18849.

7 (*a*) S. Tsuzuki, K. Honda, T. Uchimaru, M. Mikami and K. Tanabe, *J. Am. Chem. Soc.*, 2000, **122**, 3746; (*b*) M. Nishio, Y. Umezawa, K. Honda, S. Tsuboyama and H. Suezawa, *CrystEngComm*, 2009, **11**, 1757.

8 (*a*) L. Duan, Z.-H. Wu, J.-P. Ma, X.-W. Wu and Y.-B. Dong, *Inorg. Chem.*, 2010, **49**, 11164; (*b*) L. Fan, M. Xue, Z. Kang, G. Wei, L. Huang, J. Shang, D. Zhang and S. Qiu, *Microporous Mesoporous Mater.*, 2014, **192**, 29.

9 (*a*) G.-W. Zhang, P.-F. Li, Z. Meng, H.-X. Wang, Y. Han and C.-F. Chen, *Angew. Chem., Int. Ed.*, 2016, **55**, 5304; (*b*) C.-F. Chen and Y. Han, *Acc. Chem. Res.*, 2018, **51**, 2093; (*c*) L.-P. Yang, W.-E. Liu and W. Jiang, *Tetrahedron Lett.*, 2016, **57**, 3978; (*d*) G.-B. Huang, W.-E. Liu, A. Valkonen, H. Yao, K. Rissanen and W. Jiang, *Chin. Chem. Lett.*, 2018, **29**, 91; (*e*) L.-P. Yang, X. Wang, H. Yao and W. Jiang, *Acc. Chem. Res.*, 2020, **53**, 198; (*f*) G. Huang, Z. Chen, X. Wei, Y. Chen, X. Li, H. Zhong and M. Tan, *Chin. J. Org. Chem.*, 2020, **40**, 614.

10 (*a*) J.-R. Wu, A. U. Mu, B. Li, C.-Y. Wang, L. Fang and Y.-W. Yang, *Angew. Chem., Int. Ed.*, 2018, **57**, 9853; (*b*) P. Della Sala, R. Del Regno, C. Talotta, A. Capobianco, N. Hickey, S. Geremia, M. De Rosa, A. Spinella, A. Soriente, P. Neri and C. Gaeta, *J. Am. Chem. Soc.*, 2020, **142**, 1752; (*c*) X.-N. Han, Y. Han and C.-F. Chen, *J. Am. Chem. Soc.*, 2020, **142**, 8262; (*d*) S.-N. Lei, H. Xiao, Y. Zeng, C.-H. Tung, L.-Z. Wu and H. Cong, *Angew. Chem., Int. Ed.*, 2020, **59**, 10059.

11 (*a*) X. Wu, X. Han, Q. Xu, Y. Liu, C. Yuan, S. Yang, Y. Liu, J. Jiang and Y. Cui, *J. Am. Chem. Soc.*, 2019, **141**, 7081; (*b*) Y. Ohishi, M. Murase, H. Abe and M. Inouye, *Org. Lett.*, 2019, **21**, 6202; (*c*) R. Ning, H. Zhou, S.-X. Nie, Y.-F. Ao, D.-X. Wang and Q.-Q. Wang, *Angew. Chem., Int. Ed.*, 2020, **59**, 10894; (*d*) T. Hong, Z. Zhang, Y. Sun, J.-J. Tao, J.-D. Tang, C. Xie, M. Wang, F. Chen, S.-S. Xie, S. Li and P. J. Stang, *J. Am. Chem. Soc.*, 2020, **142**, 10244.

12 Both enantiomers of H_8-BINOL are available with list prices of less than \$5 (USD) per gram. For example, www.bldpharm.com, accessed May 2021.

13 K. Xu, Z.-Y. Zhang, C. Yu, B. Wang, M. Dong, X. Zeng, R. Gou, L. Cui and C. Li, *Angew. Chem., Int. Ed.*, 2020, **59**, 7214.

14 T. Ogoshi, T.-a. Yamagishi and Y. Nakamoto, *Chem. Rev.*, 2016, **116**, 7937.

15 (*a*) K. Jie, Y. Zhou, E. Li and F. Huang, *Acc. Chem. Res.*, 2018, **51**, 2064; (*b*) J.-R. Wu and Y.-W. Yang, *Angew. Chem., Int. Ed.*, 2021, **60**, 1690.

16 (*a*) D. R. Stull, *Ind. Eng. Chem.*, 1947, **39**, 517; (*b*) M. C. Burguet, J. B. Monton, M. Sanchotello and M. I. Vazquez, *J. Chem. Eng. Data*, 1993, **38**, 328.